PCCP

Accepted Manuscript

ROYAL SOCIETY OF CHEMISTRY

www.rsc.org/pccp

Journal Name

ARTICLE TYPE

Cite this: DOI: 10.1039/xxxxxxxxxx

An extended DFTB-CI model for charge-transfer excited states in cationic molecular clusters : model studies versus *ab initio* calculations in small PAH clusters

Léo Dontot, Nicolas Suaud, Mathias Rapacioli, Fernand Spiegelman

Received Date
Accepted Date

DOI: 10.1039/xxxxxxxxxx

www.rsc.org/journalname

We present an extension of the constrained Density Functional Tight Binding scheme combined with Configuration Interaction (DFTB-CI) to efficiently compute excited states of molecular clusters cations and their oscillator strengths from the ground state. The present extension consists in generalizing the initial model, relying on configurations with holes in the monomers HOMOs only, to configurations involving sub-HOMO holes, allowing for the description of higher excited states. The extended scheme is benchmarked on selected energy pathways with respect to available *ab initio* and new CASPT2 reference calculations on the benzene, naphtalene and pyrene dimer cations. The ability of the model to describe the potential energy surfaces and the transition dipole moments is discussed. The vertical electronic absorption spectra of the three dimer cations are calculated and compared with the theoretical litterature and available experimental data. Finally, the electronic absorption spectra of low energy isomers of the trimer and tetramer pyrene cluster cations are also predicted.

1 Introduction

The present work is a theoretical contribution to the calculation of electronic structure of cationic polycyclic aromatic hydrocarbons (PAH) clusters. While neutral species are characterized by electrostatic or dispersion bonding, singly cationic molecular clusters are characterized by a hole in the valence shell allowing possible inter-molecular electron hopping responsible for charge delocalization and a larger stability with respect to the neutrals. Also challenging, these compounds exhibit low excited states which differ from the ground state by their charge distribution over the different units (charge transfer excited states). Such states have importance in several application fields such as photoinduced or collisionally induced charge transfer, non-adiabatic collisions with or between molecular clusters, or transport in organic-based molecular electronics. Also, photochemistry of PAH complexes and clusters is of particular interest since these species have been suggested as candidates for carbonaceous interstellar very small grains[1]. In addition, ionized species, expected to be formed under the VUV radiation, are likely to play a significant role in grains reactivity and nucleation. Aromatic cluster cations have also been investigated in various experiments[2–20]. In this context, we report, in the present work, the determination of the electronic spectra of several PAH cluster cations.

The relationship between structure and charge localization of excited states and its influence on relaxation dynamics has been widely characterized in singly ionized rare gas clusters, often considered as atomic prototypes of molecular clusters[21–28]. Most investigations were achieved within the Diatomic-In-Molecules approximation (DIM) which can also be formulated within a charge-localized Valence-Bond type scheme[29]. It was shown that charge delocalization extends over small subunit cores. Obviously, molecular clusters are more complex, exhibiting steric effects, electrostatic, dispersion and induction anisotropy, interplay between intra and inter-molecular interactions. Calculation of electronic spectra of large molecular clusters or clusters of large molecules is thus a challenge which is not fully resolved today by *ab initio* methods. Wavefunction theory (WFT) based calculations of the electronic excited structure face the problem of size scaling. Standard Density Functional Theory (DFT) and Time-Dependant versions (TDDFT) turn out to be efficient for larger systems but do not account properly for dispersion forces and fail to describe charge transfer states at least with standard functionals[30]. Despite fruitful efforts to achieve better

[a]*Laboratoire de Chimie et de Physique Quantiques (LCPQ), IRSAMC, Université de Toulouse (UPS) and CNRS, 118 Route de Narbonne, F-31062 Toulouse, France*

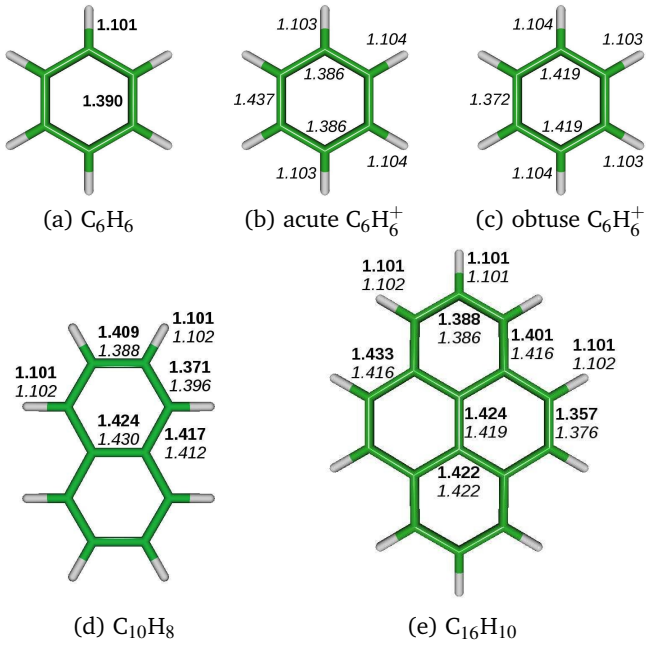

(a) C_6H_6 (b) acute $C_6H_6^+$ (c) obtuse $C_6H_6^+$

(d) $C_{10}H_8$ (e) $C_{16}H_{10}$

Fig. 1 SCC-DFTB optimized geometries (distances in Å) of benzene (a,b,c), naphthalene (d) and pyrene (e). Bold and italic fonts refer respectively to neutral and cation geometries.

scaling of WFT methods[31] and to improve the capabilities of DFT methods, namely improved functionals to correct self interaction error[32–35], hybrid CI-DFT schemes relying on the range separation[36,37], double hybrid schemes[38], improvements of TD-DFT approaches or stationary Δ_{SCF} schemes to compute the excitation energies[39], neither WFT nor DFT have yet documented investigations of cationic PAH clusters, except for dimers[40–45]. Even on dimers, few are concerned with excited states. There is thus a need for developing methods which provide a satisfactory description of excited states and are still numerically efficient for large scale simulations. Not only the vertical spectroscopy should be described but also the whole potential energy surface. Recent schemes have been proposed to approach significantly larger systems using approximate DFT schemes such as the Density Functional Tight Binding approximation (DFTB)[46–51] or TDDFTB schemes[52] and implementing some fo the mentioned improvements[53].

We have, recently, proposed an alternative scheme for the class of systems of cationic molecular cluster, based on a concept similar to that used in DIM treatments of rare gases and inspired by the work of Bouvier *et al.*[63] who developed a valence-bond model of singly charged molecular cluster cations in the rigid monomer approximation. The approach combines the Density Functional based Tight Binding method (DFTB) with a Configuration Interaction (CI) scheme[64–66], adapting the constrained DFT-CI approach[67,68] to the DFTB scheme to describe the ground state based on HOMO-holes configurations. The method scales like the number of monomers in the cluster. We have previously described the qualitative construction of the charge-transfer band restricting the CI to the HOMO holes only[66]. However, the HOMO-hole configurations may couple or even lie above configurations with holes in the near below-lying molecular orbitals generating extra low-lying states. This densification will increase with the monomer sizes. Obviously, hole-particle excitations of the neutral monomers also exist and will accordingly generate excitonic states.

Our scope here is to extend the original DFTB-CI scheme by including additional sub-HOMO hole-based excitations and investigate its ability to describe excited states of cationic molecular clusters. The lowest transitions in neutral PAHs (for instance $\sim$ 5 eV in benzene[69]) occur at higher energy than in the cationic monomer ($\sim$ 2.25 eV[54]). This justifies consideration in the DFTB-CI scheme of the cationic monomer excitations only, discarding those on neutral monomers. We then apply this scheme to investigate the low energy electronic states of selected PAH cationic clusters. The paper is organized as follows. The basics and extension of the DFTB-CI scheme are described in section 2. Section 3 presents benchmarks of DFTB-CI calculations for the cationic monomers and dimers respectively against *ab initio* CASPT2 calculations along some selected energy pathways. Finally, the DFTB-CI electronic absorption spectra of the low-lying isomers of cationic benzene and naphthalene dimers as well as pyrene clusters from dimers to tetramers are reported in section 4.

2 Method

Detailed presentation of the DFTB scheme can be found in review papers[46–51]. Additional contribution to standard DFTB can be included such as London dispersion forces as a sum over atomic pairs[70–72], corrections to atomic charges[72,73] or third order terms with respect to the density[74]. We will use here the second order DFTB (SCC-DFTB) with an empirical dispersion correction. In the present work, the interatomic hopping and overlap integrals have been corrected with a long range function[75] and an atomic polarization contribution of the form given by Iftner et al.[76] :

$$W_{pol} = \sum_a -\frac{1}{2}\alpha_a(\sum_b \mathbf{E}_{ab})^2 \quad (1)$$

was included self consistently in the DFTB scheme. The electric field is that caused on the atoms of a given monomer by the point charges of all other monomers. Each contribution $\mathbf{E}_{ab}$ is screened by a damping expression of the Aziz form, namely 1 for $R > D$ and $exp(-D/x-1)^2$ for R<D. The atomic polarisabilities were taken as 11.35 and 4.5 a_0^3 for C and H respectievely and a unique cutoff radius D=3.704 Åwas used for all pairs.

DFTB-CI, as applied to charged molecular clusters[64–66], is based on an ansatz for the ground state wavefunction as a superposition of configurations Φ_I, each one characterized by a charge localization on a given monomer I, namely

$$\Psi_0^+ = \sum_{I=1}^{M} b_0^I \Phi_I \quad (2)$$

Each configuration Φ_I results from a DFTB energy minimization with a charge localization constraint on unit I, via a Lagrange

Monomer	method	ΔE_0^{rel}	ΔE^{split}	ΔE f	ΔE (f)	ΔE (f)
$(C_6H_6)^+$				$^2E_{2g}$	$^2A_{2u}$	
	DFTB-CI			1.75	2.51 (0.213)	
	CAS(9/10)PT2/B4			2.43	2.84 (0.025)	
	CAS(9/10)PT2/B2			2.47	2.81 (0.025)	
	CAS(9/10)PT2/B1			2.54	2.83 (0.025)	
	EOM-IP-CCSD(T)[(a)]			2.88	3.33 (0.073)	
	DFTB-CI symmetric	-0.03		1.81	2.44 (0.212)	
	DFTB-CI acute	-0.15	0.45	1.99 / 2.11	2.68 (0.226)	
	DFTB-CI obtuse	-0.14	0.45	1.98 / 2.09	2.66 (0.225)	
	CAS(5/6)PT2/B1 acute		0.43		2.99	
	CAS(5/6)PT2/B1 obtuse		0.44		2.99	
	Exp. [(b)]			2.25	2.85	
$(C_{10}H_8)^+$				$^2B_{1u}$	$^2B_{3g}$	$^2B_{2g}$ (*)
	DFTB-CI			0.72	1.65 (0.249)	2.57 (0.214)
	CAS(9/10)PT2/B1			0.77	1.90 (0.056)	2.91 (0.018)
	DFTB relaxed	-0.08		0.95	1.77 (0.255)	2.71 (0.216)
	Exp[(c)]				1.84 (6.4×10^{-4})	2.72 (2×10^{-5})
	Exp.[(d)]				1.85	
	Exp.[(e)]				1.85 (0.052)	2.72 (0.010)
	Exp.[(f)]			0.73	1.93	2.70
	Exp.[(g)]				1.84	2.69
$(C_{16}H_{10})^+$				$^2B_{2g}/\Sigma$	$^2B_{1u}/\Pi_u$	^2A_u
	DFTB-CI			0.87	1.76 (0.146)	1.76 (0.380)
	CAS(15/16)PT2/B2			0.89	1.63 (0.026)	1.98 (0.043)
	TD-DFT[(h)]			0.85	1.55 (0.015)	2.01 (0.018)
	QCFF/PI[(i)]			1.17	1.79 (061)	1.97 (0.001)
	DFTB relaxed	-0.06		1.06	1.86 (0.159)	1.87 (0.390)
	Exp. [(j)]				1.58 (0.005)	1.74 (0.003)
	Exp. [(k)]			0.85	1.59	1.88

Table 1 Transition energies (ΔE in eV) and oscillator strengths (f in atomic units) from ground to excited states of the benzene, naphthalene and pyrene cations. By default, the geometries are those of the neutral monomer optimized in SCC-DFTB. Data for the relaxed cationic monomers (specifically indicated as symmetric, acute, obtuse or relaxed) and relaxation energies ΔE_{rel} (with reference to the energies of the non relaxed cation at the geometries of neutrals) are also given. Δ_E^{split} is the excitation energy resulting from he Jahn-Teller stabilization of benzene. (a) Ref.[43]; (b) Ref.[54] (photoionization); (c) Ref.[55](Ne matrix); (d) Ref[56] ; (e) Ref.[57] ; (f) Ref.[58] neutral geometry ; (g) Ref.[58] cation geometry ; (h) Hirata *et al.*[59]; (i) Negri and Zgierski[60]; (j) Vala *et al.*[61] (photoabsorption); (k) Boschi and Schmidt[62] (photoionization). (*In naphtalene,) two electronic forbidden states, with holes in σ HOMO-3 and HOMO-4 orbital in DFTB-CI and transition energies 2.28 2.54 eV in neutral geometry and 2.48/ 2.66 eV are not presented in the table.

parameter V_I incorporated in the DFTB hamiltonian H^{DFTB} :

$$H^I = H^{\mathrm{DFTB}} + V_I P_I \tag{3}$$

where P_I is a projector of the electronic density on unit I and V_I the Lagrange parameter searched iteratively to reach the target number N_I of electrons on monomer I. The resulting KS orbitals ϕ_i^I define configurations Φ_I and the corresponding energies E_I, identified with the diagonal elements of the CI hamiltonian H_{II}.

The off-diagonal elements, describing the hole hopping between monomers I and J, are calculated following the approach of Wu *et al.*[67,68] :

$$H_{IJ} = \frac{1}{2}(E_I + E_J + N_I V_I + N_J V_J) S_{IJ}$$

$$-\frac{1}{2}(V_I \langle \Phi_I | P_I | \Phi_J \rangle + V_J \langle \Phi_I | P_J | \Phi_J \rangle) \tag{4}$$

where $S_{IJ} = <\Phi_I|\Phi_J>$. The resolution of the secular equation corresponding to the CI hamiltonian expressed in a non-orthogonal basis provides orthogonal ground and excited states Ψ_m^+ as well as their eigenvalues E_m^+.

The quality of the charge resonance excited states obtained in the aforementioned approach may be insufficient due to the small basis of charge localized configurations, and states involving local excitations are obviously absent. In the present work, we extend the basis of the CI matrix to introduce charge localized excited configurations. Starting from the charge localized wavefunction Φ_I, we define a single hole excitation with respect to the lowest energy configuration (using second quantization notation) :

$$\Phi_{Ik} = a_{Ik}^{\dagger} a_{Ih} \Phi_I \tag{5}$$

where the hole is now created in orbital k localized on fragment I. At this point, a comment about the localization procedure should be made. The localization process which is carried out using the Lagrange multiplier is a localization criterion about the density of charge on a given monomer. It is not a per-orbital criterion. This means that the excited configurations Φ_{Ik} $(k \neq h)$ might be affected by partial delocalization, due to the replacement of the hole orbital. It turns out that, in the present applications, the charges Q_{Ik} of the excited configurations Φ_{Ik}, calculated within the Mulliken definition, remain mainly on molecule I with respect to the projection criterion $0.8 < Q_{Ik} < 1.2$. This is important in view of the self interaction error which is quenched in a localized description, but would pollute the calculation of the energies in case of significant delocalization[33].

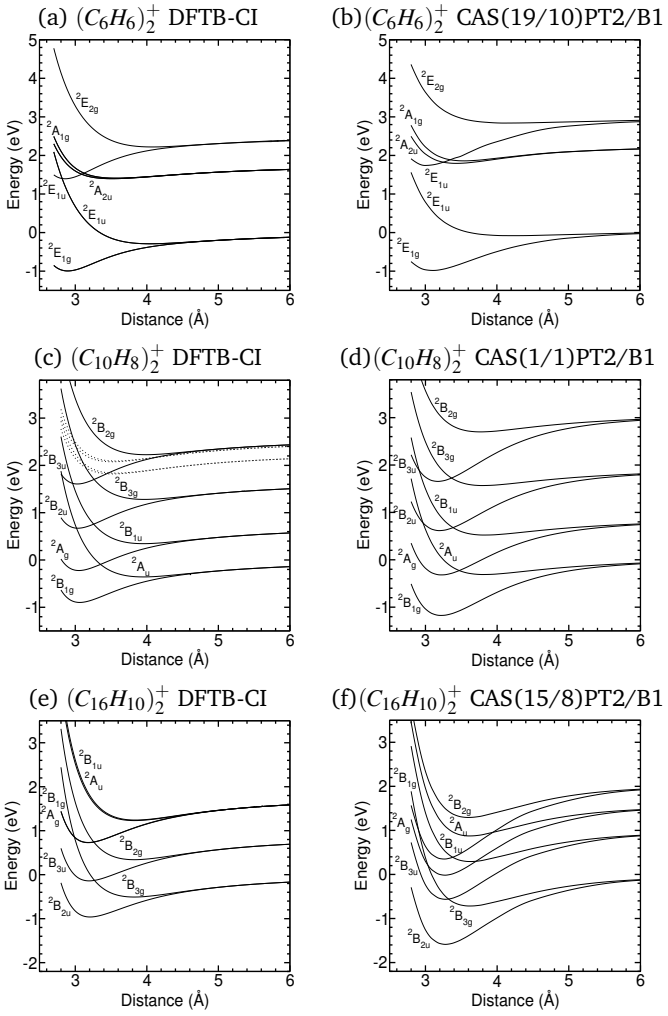

Fig. 2 Potential energy profiles along the inter-molecular separation in the sandwich approach for the benzene, naphthalene and pyrene dimer cations obtained with DFTB-CI (a),(c), (e) and CASPT2 (b),(d),(f) methods.

The calculation of the CI matrix elements in the extended basis set Φ_{Ik} requires some ansatz due to the fact that the excited configurations are not eigenvalues of any specific hamiltonian. The energies of Φ_{Ik} (the CI diagonal matrix elements) are calculated without orbital relaxation (frozen orbitals approximation) at the DFTB level with the corresponding excited configuration densities. The second one concerns the off-diagonal elements, for which we have assumed similar formulas as for the calculation of the hopping integrals as in the HOMO band, namely

$$H_{Ik,Jl} \simeq \frac{1}{2}(E_{Ik}+E_{Jl}+N_I V_I+N_J V_J)S_{Ik,Jl} - \frac{1}{2}(V_I\langle\Phi_{Ik}|P_I|\Phi_{Jl}\rangle + V_J\langle\Phi_{Ik}|P_J|\Phi_{Jl}\rangle) \quad (6)$$

which is only exact when both holes are in the HOMO orbitals. In the case $I=J$ and $k\neq l$, the coupling matrix elements are set to zero.

The transition dipole moment from state p to state m can be derived from the expression :

$$\mathbf{D}_{pm} = <\Psi_p^+|\mathbf{D}|\Psi_m^+> \quad (7)$$

In the complete development of this formula, we make use of atomic transition charges like in the time-dependent DFTB formulation[52]. The oscillator strength of the transitions from the ground state ($p=0$) to excited state m is then computed using the Franck-Condon approximation

$$f_{0m} = \frac{2}{3}\Delta E_{0m}|\mathbf{D}_{0m}|^2 \quad (8)$$

where ΔE_{0m} is the transition energy $E_m^+ - E_0^+$. All developments reported in the previous section have been implemented within an experimental version of the deMonNano code[77].

Some *ab initio* data are available in the literature for monomers and dimers. Nevertheless, in order to handle a common set of reference data, we have achieved new *ab initio* calculations for the cationic monomer and dimer species at the CASSCF and CASPT2 level using the MOLCAS package[78–80]. Calculation of BSSE via the ghost orbital methods may be delicate for excited states, especially when using perturbation theory. Then, we checked the stability of the results upon the basis sets on the benzene dimer cation with basis sets of increasing quality. Basis B1 describes the carbon and hydrogen atoms with $3s2p1d$ and $2s$ ANO-RCC sets[81,82] respectively, B2 is extended to $4s3p2d$ and $2s1p$, B3 to $5s4p2d1f$ and $3s1p$ and finally B4 to $6s5p3d2f1g$ and $4s2p1d$ (those sets are the corrected versions recently reported by the MOLCAS team, see MOLCAS web site). Only the two first basis sets could be used for the pyrene dimer cation, depending on the dimension of the CAS. For each application, the largest feasible compromise between basis set and CAS is reported. The basis and the CAS dimensions will be indicated together with the basis sets. Optimized MOs originate from a CASSCF procedure which also determines the zeroth-order description of the states. The main effects of excitations out of the active orbitals are accounted at second order of perturbation theory via the CASPT2 scheme[83–85].

3 Benchmarks on PAH monomer and dimer cations

The scope of the present section is to benchmark the present DFTB-CI results obtained for benzene, naphthalene and pyrene cation dimers for which *ab initio* calculations are still either available or feasible.

We first analyze the excitation energies of the cationic monomers, which will determine the asymptotic positions of the dimer energies and thus also influence the excitation energies of clusters, since they appear in the diagonal of the CI matrix. We have first determined the geometries of the neutral (namely D_{6h} for benzene, D_{2h} for naphthalene and pyrene) and cationic monomers with standard SCC-DFTB optimization (Fig. 1). The vertical excitation energies at these geometries are reported in Table 1.

Benzene in D_{6h} symmetry exhibits the following molecular or-

System	method	D_e	R_e	D_e	R_e	D_e	R_e	D_e	R_e	D_e	R_e	D_e	R_e	D_e	R_e	D_e	R_e
$(C_6H_6)_2^+$		$^2E_{1g}$		$^2E_{1u}$		$^2A_{2u}$		$^2A_{1g}$		$^2E_{1u}$		$^2E_{2g}$					
	DFTB-CI	0.99	2.90	0.29	4.04	0.36	3.57	0.34	3.65	0.97	3.12	0.29	4.08				
	CAS(19/10)PT2/B1	0.98	3.11	0.08	4.24	0.41	3.44	0.35	3.55	1.31	3.00	0.21	4.09				
$(C_{10}H_8)_2^+$		$^2B_{1g}$		^2A_u		^2A_g		$^2B_{1u}$		$^2B_{2u}$		$^2B_{3g}$		$^2B_{3u}$		$^2B_{2g}$	
	DFTB-CI	0.90	3.06	0.36	3.96	0.94	3.04	0.37	3.95	0.98	3.03	0.37	3.96	0.97	3.03	0.35	3.99
	CAS(1/1)PT2/B1	1.17	3.21	0.31	3.80	1.14	3.23	0.30	3.81	1.23	3.19	0.28	3.79	1.39	3.17	0.34	3.77
$(C_{16}H_{10})_2^+$		$^2B_{2u}$		$^2B_{3g}$		$^2B_{3u}$		$^2B_{2g}$		^2A_g		$^2B_{1u}$		$^2B_{1g}$		^2A_u	
	DFTB-CI	0.96	3.20	0.51	3.82	1.01	3.19	0.53	3.82	1.04	3.18	0.53	3.83	1.03	3.18	0.52	3.84
	CAS(15/8)PT2/B1	1.59	3.28	0.72	3.62	1.57	3.28	0.71	3.62	1.60	3.27	0.71	3.61	1.71	3.26	0.77	3.59
	CAS(1/1)PT2/B1	1.58	3.28	0.72	3.62	1.56	3.28	0.71	3.62	1.59	3.27	0.70	3.61	1.71	3.26	0.77	3.59
	CAS(1/1)PT2/B2	1.65	3.28	0.78	3.60	1.63	3.28	0.77	3.62	1.65	3.28	0.77	3.60	1.77	3.27	0.83	3.59
	CAS(1/1)PT2/B3	1.51	3.29														

Table 2 Stabilization energies (eV) and minimal energy distances (Å) for ground and excited states of cationic benzene, naphthalene and pyrene dimers in sandwich geometries.

bital picture: the highest occupied orbitals consist of a twofold degenerate π HOMO, a twofold degenerate σ HOMO-1, a non-degenerate fully bonding π HOMO-2. The virtual orbitals are their antibonding counterparts, namely a twofold degenerate π^* LUMO, a twofold degenerate σ^* LUMO+1 and another π^* LUMO+2. The lowest excitation energies in the cation actually correspond to $\sigma \rightarrow \pi$ dipole-forbidden transitions and the next lowest to a dipole-allowed $\pi \rightarrow \pi$ transition. The two lowest DFTB-CI transitions in the cation are smaller (1.75 and 2.51 eV) than the *ab initio* values (2.43 and 2.84 eV from CASPT2; 2.88 and 3.33 eV for EOM-IP-CCSD(T)[43]. The Jahn-Teller (JT) effect in the benzene cation is accounted for by DFTB, yielding two D_{2h} isomers, namely an acute form ($^2B_{3g}$) and an obtuse form ($^2B_{2g}$) on the two respective energy surfaces originating from the conical intersection. Theses isomers, stabilized by 0.15 and 0.14 eV respectively with respect to the energy at the ground state geometry, are quasi-degenerate. As a result, a transition occurs at low energies, 0.45 eV for both acute and obtuse geometries. The other transitions from the ground state are slightly increased by 0.15-0.25 eV, presenting a small error with respect to the CASPT2 values ($\sim$ 0.3 eV). State $^2E_{2g}$ is split into a doublet feature with a separation of $\simeq$ 0.1 eV.

In the naphthalene case, out of the five highest occupied orbitals, HOMO-3 and HOMO-4 are σ MOs, the other three being π orbitals. All five lowest unoccupied orbitals are π^* MOs. At the neutral geometry, the DFTB transition energies towards the lowest excited states, namely 0.72 and 1.65 eV, are slightly smaller than the CAS(9/10)PT2 values, 0.77 and 1.90 eV respectively, the experimental values being 0.73 and 1.93 eV, respectively[58]. Relaxation results in a stabilization of -0.08 eV and increases the transition energies by 0.10-0.25 eV.[61,86–89] The case of pyrene is very similar to that of naphthalene. At the neutral geometry, the lower transition energy is consistent with the CASPT2 result. At the cation geometry, the transition energies are in good agreement with previous TDDFT or QCFF/PI results (see Table 1) as well as with experimental data[61,62,90], namely 0.87 eV for the first transition, in the range [1.5-1.6] eV for the second excitation and in the range [1.7-1.9] eV for the third one. However, the DFTB third transition in pyrene is underestimated, leading to an fortuitous quasi-degeneracy with the second one. This degeneracy is lifted by relaxation which stabilizes the ion by 0.06 eV and increases the transition energies.

Oscillator strengths f for the dipolar transition from the ground state are reported in Table 1. In the D_{6h} benzene cation, the transition towards the first (doubly degenerate) excited state $^2E_{2g}$ is forbidden due to symmetry. For the oscillator strengths towards state $^2A_{2u}$, we observe that the DFTB-CI value (0.213) is much larger than the CASPT2 determination (0.025). In the case of the pyrene cation, two states are dipolar-allowed, i.e. $^2B_{1u}$ and ^2A_u. The CAS(15/16)PT2 calculation in which the $\pi \rightarrow \pi^*$ excitations are considered variationally exhibits much smaller oscillator strengths than CAS(15/8)PT2, where only the $\pi \rightarrow \pi$ excitations are considered variationally. One should note that CASPT2 is a contracted method, the weights of the zeroth order configurations are not modified in the perturbation, which may affect the CAS(15/8)PT2 cases. DFTB-CI provides values similar to those of CAS(15/8)PT2, consistent with the absence of single excitations toward π^* orbitals. The situation is quite similar in naphtalene. For all three molecular cations, the analysis of the *ab initio* calculations stresses the importance of a wavefunction including at least partly the dynamical correlation in the determination of the oscillator strengths. To conclude this discussion, while the monomer transition energies remain reasonable with respect to experiments, the oscillator strengths still present strong fluctuations in the various methods and with respect to experiment. One has therefore to keep in mind, when analyzing the results for clusters, that the accuracy of the positions of the asymptotic states (*i.e.* the cationic monomer excitations) will influence directly the accuracy of the cluster cations excited states. Actually, this argument lead Pieniazek *et al.*[43] to phenomenologically shift their EOM-IP-CCSD(T) adiabatic dissociation profiles in $(C_6H_6)_2^+$ by their asymptotic error ($\sim$ 0.5 eV) for some of the excited states. The analysis of the present CAS results shows that the two first excitations correspond mostly to a single-hole excitation whereas the third one involves several single-hole excitations for which non-dynamical correlation in the valence space is expected to be

more important. The generally observed underestimation of the present DFTB-CI transition energies is more likely to be explained by errors resulting from the DFTB parametrization used, since inclusion of more single or higher excitations are likely to still decrease the transition energies. The structural and energetical changes between neutral and ion tend to decrease with monomer size.

We now present DFTB-CI calculations of cationic benzene, pyrene and naphthalene dimers on significant pathways on the potential energy surface. Along those pathways, the molecules are kept frozen at their neutral geometries (sandwich, T-shaped and rotation). Figure 2 presents the DFTB-CI and CASPT2 energy profiles along the sandwich geometry dissociation path while Table 2 reports the stabilization energies and the minimal energy distances of the excited states along this path. Several general features can be noticed : (i) the DFTB-CI energies converge to the sum of the energies of the monomers at the frozen geometry. This was expected since DFTB-CI is expressed in a localized charge description; (ii) DFTB-CI accounts for the large splitting of states with $\pi \rightarrow \pi$ excitation, much larger than the splitting of states with $\pi \rightarrow \sigma$ states (for instance $^2A_{2u}$ and $^2A_{2g}$ states in the benzene dimer). This is consistent with the results of CASPT2; (iii) The DFTB-CI excited states in the sandwich approach seem systematically less bound than the CASPT2 states. This may be due to an overestimation of the DFTB inter-molecular repulsion *vs* dispersion or polarization. It can also be due to unsatisfactory distance evolution of the hopping integrals and/or overlaps. Actually, the degeneracy breaking occurs at too short distances. In another context, Kubar *et al.* [91] computed charge transfer hopping integrals within a coarse grain DFTB-based scheme and found that the hopping hole transfer switch on at too short range. This effect was attributed to the conventional compression radii used in DFTB parametrization, which could also contribute to the errors in the present approach; (iv) In pyrene, four states correlated with the $^2B_{1u}$ and the ^2A_u of the cationic monomer are quasi-degenerate, in direct relationship with the accidental quasi-degeneracy of the DFTB states observed for the isolated monomer. This explains the the main differences between Fig. 2.(e) and Fig. 2.(f)

At this point, it may be noticed that the present calculations along the inter-molecular dissociation coordinates show that the scheme, positionning the antibonding charge transfer state clearly below the intramonomer bonding excited state, seems erroneous for the naphtalene and pyrene dimer cations. This occurs for the latter systems above the ground state equilibrium geometry, due to crossings between states generated by various types of excitations. This may play a role in the interpretation of photodissociation experiments.

In order to provide a benchmark for which the two molecules are not equivalent, and the diagonal terms in the CI matrix are non-degenerate, we investigated the dissociation pathway for a naphthalene dimer cation presenting T-shape geometry (see Figure 3). It can be seen that DFTB-CI succeeds in reproducing the CASPT2 main trends, namely (i) the smaller splittings with respect to those obtained for the sandwich approach and (ii) the smaller splitting of the dimer states correlated with the first

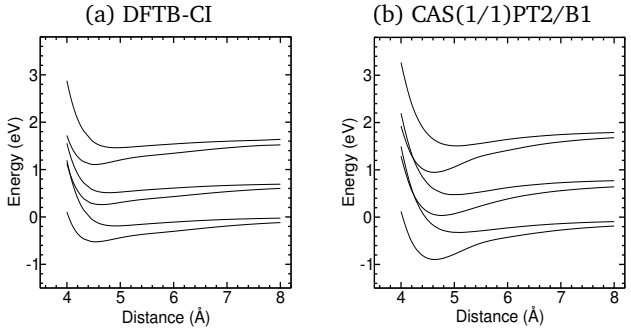

Fig. 3 Potential energy profiles along the inter-molecular distance (distance between the molecule centers) in T-shape approach for $(C_{10}H_8)_2^+$ with DFTB-CI (a) and CASPT2 (b).

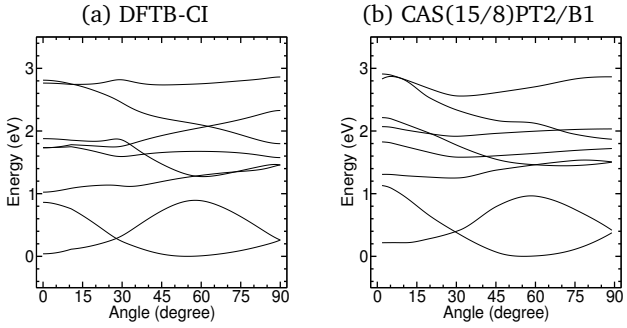

Fig. 4 Potential energy profiles along the twist angle for $(C_{16}H_{10})_2^+$ with DFTB-CI (a) and CASPT2 (b).

monomer excited state with respect to those correlated with the the ground state and second monomer excited state. Again, the minimal energy distance and bonding energy are underestimated.

As an additional benchmark, we have represented in Fig. 4 the DFTB-CI and CASPT2 energy profiles for the cationic pyrene dimer, varying now the twist angle θ around the inter-molecular axis (the two molecules rotating on top of each other, keeping the molecular planes parallel). The DFTB-CI calculations involving four single-hole configurations are quite comparable with the CASPT2 results.

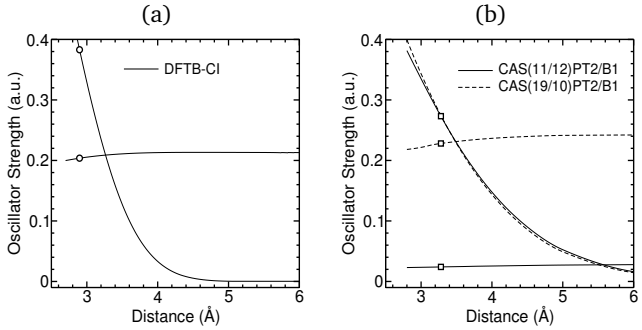

Fig. 5 Evolution of the oscillator strengths as a function of the inter-molecular distance (Å) for the first and second lowest electronic transitions in the benzene dimer cation along the sandwich approach with DFTB-CI (a) and CASPT2/B1 (b) calculations

We now discuss the validity of the DFTB-CI approach to re-

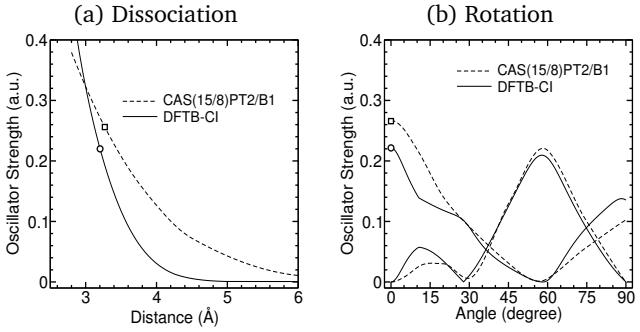

Fig. 6 (a) Evolution of the oscillator strengths of the first and second electronic transitions in the pyrene dimer cation with DFTB-CI and CASPT2 calculations. (a) as a function of the inter-molecular distance (Å) for the cationic pyrene dimer in the sandwich geometry (b) as a function of the twist angle (degrees) at an inter-fragment distance of 3.05 Å (DFTB-CI) and 3.26 Å (CAS(15/8)PT2/B1).

produce the oscillator strengths of the dipolar transitions from the ground state. Fig. 5 represents the evolution of the oscillator strengths for the benzene dimer cation in the sandwich approach, varying the inter-molecular distance. The first one corresponds to excitation $^2E_{1g} \rightarrow ^2 E_{1u}$, namely from the bonding to the antibonding state correlated with the ground state benzene cation. The corresponding dipole moment is zero at dissociation and increases rapidly at short distances, in consistency with the inter-molecular nature of this excitation. This is also in agreement with the CASPT2 calculations. Neither the size of the basis set, nor the size of the CAS space affects strongly the various CASPT2 oscillators strengths, which are all almost superimposed in the figure. One may observe, that the increase of the DFTB oscillator strengths starts at smaller inter-molecular distance than in the *ab initio* calculations. This is to be correlated with the too short equilibrium distances found for the energy pathways and the too small splittings. The other excitation is mainly an intra-molecular excitation correlated with excitation to the $^2A_{2u}$ state of the monomer cation, and is asymptotically allowed for large inter-molecular distance. Its oscillator strength is almost equal to that in the monomer treated with a corresponding calculation. CAS(11/12)/B1 and CAS(11/12)/B2 provide identical oscillator strengths with a magnitude in the range 0.025-0.026 consistent with the CAS/B2 results on the benzene cation. In contrast, the oscillator strength in CAS(19/10)/B1 is close to 0.25, overestimated by a factor 10. CAS(19/10) does not include the π^* MO. The DFTB-CI model, which lacks excitation towards the π^* monomer orbitals yield an almost constant oscillator strength ($\sim$ 0.2), close to the CAS(19/10)/B1 value. This is in line with the ability of the various CAS spaces to describe the monomer cation intensities. It can be concluded that: i) the calculation of intra-molecular oscillator strengths do necessitate CAS (full valence π) wavefunctions while CAS spaces based on occupied π MOs only are sufficient to correctly evaluate the inter-molecular excitation oscillator strengths.

Figure 6 reports oscillator strengths obtained along inter-fragment separation of the pyrene sandwich dimer for the lower bonding to antibonding state transition ($^2B_{3g} \rightarrow ^2B_{2u}$) with CAS(15/8)PT2 and DFTB-CI. These results are quite similar to those obtained for the equivalent transition in the benzene dimer cation. Figure 6(b) shows the evolution of the oscillator strengths along a rotation pathway of two superimposed pyrene molecules. Excitations from $^2B_3$ to the two $^2B_2$ states, namely from the ground state to the two lowest excited states for $\theta \leq 30$ degrees, respectively, are represented. For $\theta = 0$ degree, the states are correlated with $^2B_{3g}$, $^2B_{2g}$ and $^2B_{2u}$, respectively. One transition has a null value for $\theta = 0$ degree (it corresponds to the $^2B_{3g} \rightarrow ^2B_{2g}$ forbidden transition in the D_{2h} symmetry). It is also null for $\theta \simeq 27^\circ$ and 90 degrees (due to crossing between the two states) and presents two maxima at $\theta \simeq 15$ degrees and $\theta = 57$ degrees. The oscillator strength of the other transition decreases between $\theta = 0$ degree ($^2B_{3g} \rightarrow ^2B_{2u}$ in the D_{2h} symmetry) and $\theta = 57$ degrees. For $\theta = 0$ degree, the first (forbidden) transition corresponds to a combination of intra-molecular excitations while the second one is an inter-molecular excitation from the bonding to the antibonding combination of the molecular HOMOs. As shown above, CASPT2 calculations not based on a CAS containing the whole valence π MO do not correctly evaluate the intra-molecular transition oscillator strength. Since the symmetry breaking due to rotation induces mixing of intra- and inter-molecular excitations, the evaluation of the oscillator strengths should not be accurate. Nevertheless, two reasons allow us to argue that these evaluations are still meaningful: (i) the first excited state $^2B_{3g}$ remains high in energy and avoids strong mixing with the lowest one; (ii) the two $^2B_2$ states consist of a mixing of an inter-molecular excitation (correctly estimated) with a forbidden intra-molecular excitation, that should remain very small during the rotation. This assumption is supported by the observation that the sum of the oscillator strengths of the two transitions is almost constant along the rotation angle. We can see that despite a rather intricated electronic situation, the DFTB-CI oscillator strengths evolutions are consistent with the results obtained at the CASPT2 level.

4 Relaxed structures and absorption spectra of cationic clusters

As a direct application of the DFTB-CI approach, we have computed the spectra of the low energy isomers found for cationic benzene, naphthalene and pyrene dimers and also those of small clusters, namely the cationic pyrene trimers and tetramers.

Due to the PES complexity (mainly caused by a large number of degrees of freedom), we used a global exploration algorithm combined with local optimization to find the most stable structures : (i) a parallel tempering Monte Carlo simulation[92] in the rigid monomer approximation is achieved from which we select $\sim$ 1000 low energy structures. This part requires an extensive number of single point calculations, typically 10^8 for each system and a set of 10 to 20 temperatures in the range 10 K-700 K; (ii) the selected geometries are optimized with an all-atom conjugated gradient algorithm. The exploration is performed at the DFTB-CI level without considering local excitations, as their introduction has a minor effect on the ground state energy. This allows in particular the use of analytical gradients[65] for the final conjugated gradient optimizations.

From the previous discussion on the quality of the spectra obtained from the DFTB-CI, one has to keep in mind that only the lowest excited states are reliable and will be discussed here, although the whole spectrum is presented. As already discussed above for monomer and dimer oscillator strengths, intensities of transitions to the states where the monomer HOMO and HOMO-1 configurations are mainly populated can be reliable (symbolized in the following figures by squares), while intensities of transition to the states with an important weight on monomers HOMO-2 or HOMO-3 configurations are expected to be overestimated (triangles).

Two structures have been found for the benzene dimer cation. The most stable isomer (2a) is a sandwich structure, displaced along an axis joining opposite apexes of the molecules and has a binding energy of 1.17 eV. In this isomer, the benzene monomer geometries are close to the acute structure obtained for the cationic isolated monomer. The first transition, with an energy of 1.35 eV, has a strong intensity (0.324). The second isomer (2b) is a superimposed sandwich with an angle between the molecular planes of about 30 degrees. The benzene molecules are, in this case, close to the obtuse cationic monomer. The full relaxation of the benzene dimer cation structure via CASSCF/CI methods was carried out by Myoshi et al.[42] and later on by Kryachko[44] using DFT/B3LYP (S and D sandwich isomers). Both isomers found here with DFTB-CI correspond to those found in those *ab initio* optimizations. The structural excitation towards isomer (2b) being 27 meV in DFTB-CI, to be compared with 20 meV at the DFT/B3LYP level[44]. The experimental values for the binding energies lie in the range 0.6-0.9 eV[2,8–15]. The DFTB-CI binding energies (1.17/1.15 eV) are larger than those of Kryachko (0.72/0.71 eV), the latter being consistent with the two experimental determinations 0.76 eV[14] or 0.78 eV[15]. Notice from table 2 that the CASPT2 binding seems larger, at least along the dissociation path (for the non-relaxed structures). A number of experimental studies have been concerned with the spectroscopy of the benzene dimer cation[14–16]. The photodissociation spectra have been investigated, revealing five peaks at 1.07, 1.35, 2.14 and 2.82 eV. The two first peaks were assigned to charge transfer excitations. Our calculated spectra for isomers (a) and (b) are at respectively 1.35 and 1.15 eV. This might be compatible with the contributions from both isomers in the experimental peaks. Additional transitions are found around 2 eV (2a) and 2.4 eV (2b).

The two low-energy isomers found for naphtalene are a twisted superimposed structure (2a) (twist angle of 90 degrees), and a second structure (2b) with essentially superimposed monomers, but presenting a dihedral angle, similarly to structure (2b) of benzene. Again, like for the benzene dimer cation, the binding energies of the present DFTB-CI isomers for the naphtalene dimer cation, respectively 1.09 eV (2a) and 0.96 eV (2b) are larger than the experimental value of 0.68 eV provided by Fujiwara et al.[17]. The DFTB-CI electronic spectra generated by both structures are not significantly different, with two neigbouring and intense transitions around 2.3 eV (2a) and 1.8 eV (2b). The charge transfer transition state was estimated experimentally around 1.05 eV[17,18] and a excited state correlated with intramonomer excitation was identified at 2.17 eV. While our calculation seems to

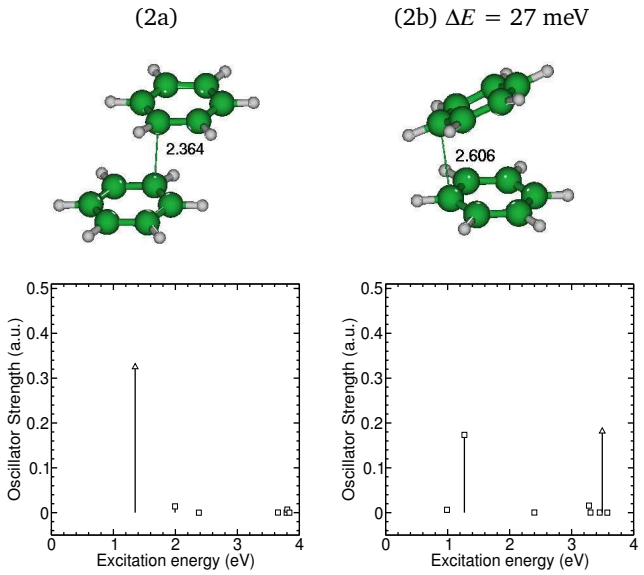

Fig. 7 Structures and spectra of low energy isomers of the benzene dimer cation (interatomic distance in Å)

be consistent for the second state, the charge transfer transition seems strongly overestimated in the present calculation. An interesting point in the naphtalene dimer cation is the presence of a low-lying transition with vanishing intensities at 1.75 and 1.3 eV in the respective isomers (2a) and (2b), related to the crossing in Fig 2 between the lowest charge transfer state and a bonding state correlated with the second monomer asymptote, namely the crossings between states ^2A_u and ^2A_g of Figs. 2 (c) and 2(d).

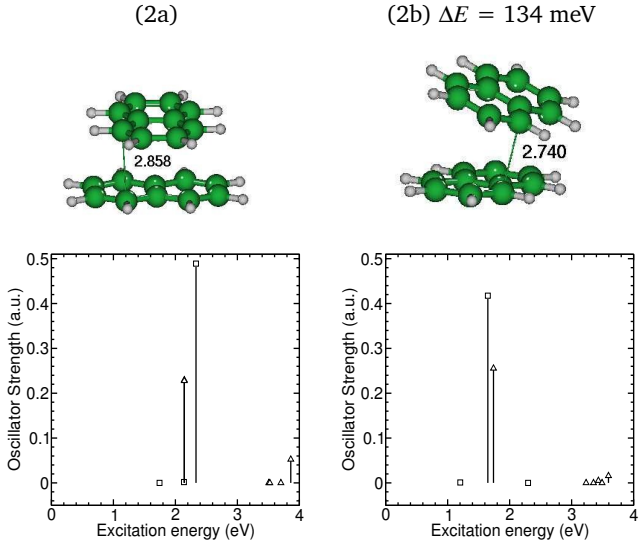

Fig. 8 Structures and spectra of low energy isomers of the naphthalene dimer cation (interatomic distance in Å)

The most stable isomer of the cationic pyrene dimer (2a) has a twisted sandwich geometry (θ=90 degrees) and the second one (2b) has a parallel-displaced structure (less stable by $\Delta E = 33$ meV). In the associated spectra, the first excited state corresponds mainly to the antibonding HOMO-hole configurations with a

System	Isomer	D_e (eV)	charge distribution (%)
$(C_6H_6)_2^+$	(2a)	1.17	50 | 50
	(2b)	1.15	54 | 46
	Exp.$^{(a)}$	0.76	
	Exp.$^{(b)}$	0.90	
$(C_{10}H_8)_2^+$	(2a)	1.09	50 | 50
	(2b)	0.96	50 | 50
	Exp.$^{(c)}$	0.68	
$(C_{16}H_{10})_2^+$	(2a)	1.01	50 | 50
	(2b)	0.98	50 | 50
$(C_{16}H_{10})_3^+$	(3a)	1.73	48 | 26 | 26
	(3b)	1.61	54 | 23 | 23
	(3c)	1.60	50 | 50 || 0
	(3d)	1.53	50 | 49 || 1
$(C_{16}H_{10})_4^+$	(4a)	2.41	26.5 | 47 | 26.5 || 0
	(4b)	2.33	12 | 37.5 | 37.5 | 12

Table 3 DFTB-CI ground state dissociation energies (eV) with respect to neutral monomer evaporation channel for relaxed benzene, naphthalene and pyrene dimer cations and relaxed pyrene trimer and tetramer cations. Experimental data are from (a) Ref.[2], (b) Ref.[12] and (c) Ref.[17]

cumulative weight of 80% in (2a) and 54% in (2b) (and a weight of 46% on configurations with HOLO-3 holes). The DFTB-CI transitions from the ground state to these states are at 1.11 eV (2a) and 0.59 eV (2b) with respective oscillator strengths 0.242 and 0.091. Experimentally, the charge transfer state is found at 0.86 eV, and three transitions to states correlated with intramonomer excitations have been found at 1.63 eV, 1.96 eV and 2.53 eV, in possible correspondance with the calculated transitions at 1.8, 2.05 and 2.2 eV for isomer (2a) or at 1.6, 1.8 and 2.53 eV for isomer (2b).

Let us notice in general that the charge transfer excited state are strongly repulsive as a function of the inter-molecular distance as illustrated in Fig. 2 at the equilibrium geometry of the ground state dimer cations. Any error on the geometry with respect to the inter-molecular coordinate could induce a strong shift of the vertical transition. Inter-molecular distances in the sandwich approaches are slightly smaller in DFTB than in CASPT2. A too short inter-molecular distance for the ground state can be seen in Fig.2 for the naphtalene and pyrene systems. Obviously, another possible cause for discrepancy remains the possibility of having missed a low-energy isomer despite the extensive search. Eventhough, the benzene and pyrene cases present distinct lines for isomers (2a) and (2b), it is difficult from the present theoretical spectra to assign the isomers in the experiments. Finally, temperature may also cause spectral broadening or shifts.

The low energy pyrene trimers and their corresponding spectra

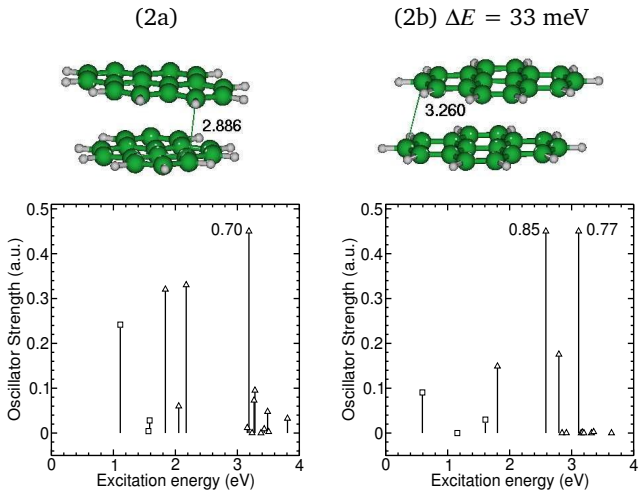

Fig. 9 Structures and spectra of low energy isomers of the pyrene dimer cation (interatomic distance in Å)

are represented in 10. The most stable structure (3a) found for the pyrene trimer cation is a stack of three twisted monomers. We also present here the stack isomer formed by three parallel-displaced fragments (3b) lying at $\Delta E = 123$ meV above the lowest energy isomer. The excitations to the first excited states at 0.81 eV (3a) and 0.71 eV (3b) present the largest oscillator strengths, respectively 0.324 and 0.310. They correspond to a charge transfer to the on-side fragments. Less stable trimer isomers can be formed around a cationic dimer core with a neutral molecule on the side : structure (3c) has a dimer core similar to the most stable cationic dimer (2a) and structure (3d) is built from a dimer similar to the parallel-displaced isomer (2b). It can be seen that the spectra of these trimers show similarities with the corresponding dimer spectra.

Tetramer isomers and their spectra are represented in Figure 11. The most stable structure (4a) is formed by a stack trimer with a monomer on the side. In the ground state, the charge is localized on the stack and the monomer is almost neutral. The structure of the trimer stack core is close to the structure of the most stable trimer (3a) and the two spectra are very similar.

Another interesting isomer is the stacked tetramer (4b), less stable by 77 meV than the most stable isomer (4a). In the ground state, the charge is delocalized over the whole stack with a charge distribution of 37.5 % for the two molecules in the center and 12 % for the molecules on edges. The first transition at 0.71 eV is intense with an oscillator strength of 0.38 and correspond to a charge transfer to the edges of the cluster, the charge of the upper state being localized at 11% on the molecules in the center and 39 % on molecules on the edges).

5 Conclusion

In this work, we have presented an original approach to access excited states of cationic molecular clusters generalizing the DFTB-CI scheme to include, not only the basic configurations with a hole in a monomer HOMO, but also configurations consisting of single hole excitations.

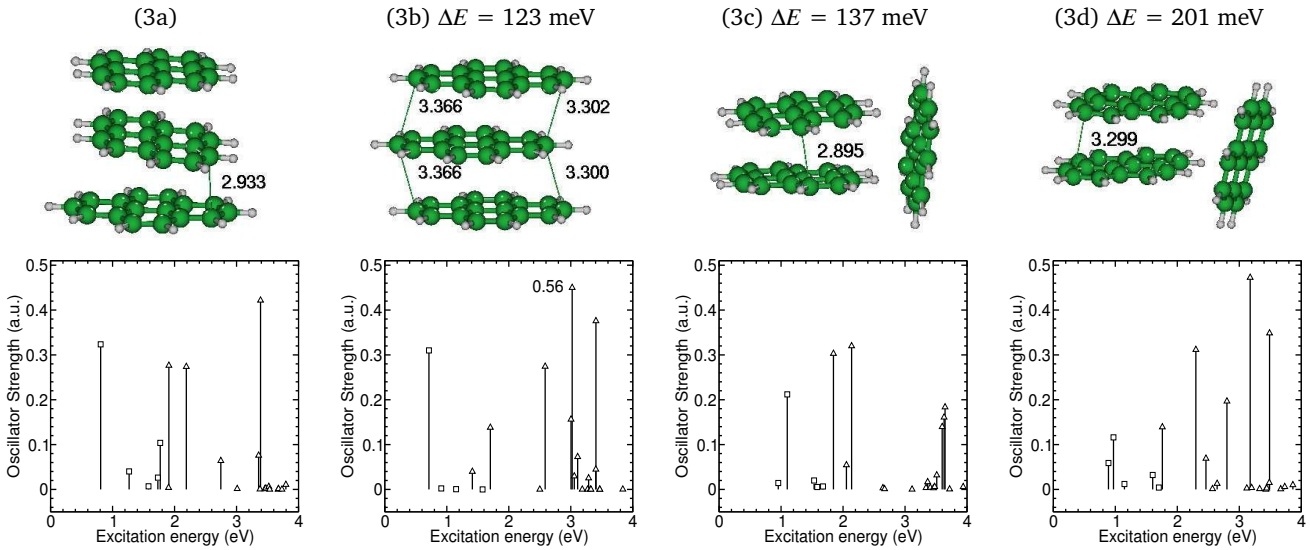

Fig. 10 Structures and spectra of low energy isomers of the pyrene trimer cation (interatomic distances in Å).

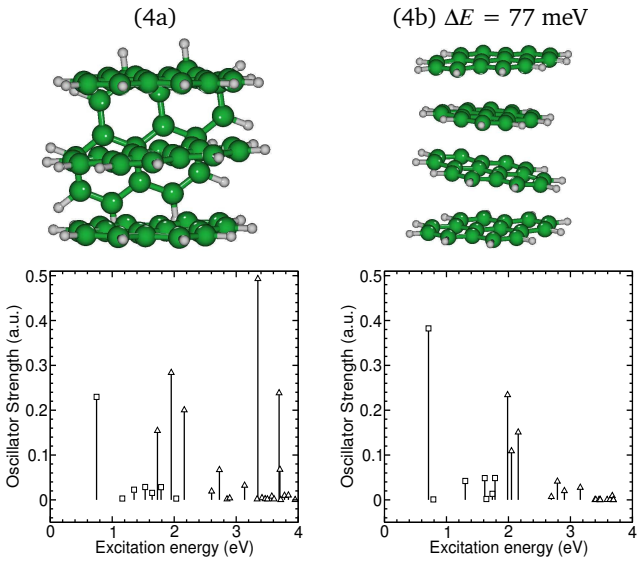

Fig. 11 Structures and spectra of low energy isomers of the pyrene tetramer cation.

In order to benchmark the results, we have compared the DFTB-CI results with *ab initio* CASPT2 reference data for dissociation and rotation pathways for benzene, naphthalene or pyrene cationic dimers. This comparison, combined with CAS wavefunction analysis, shows that the DFTB transition energies converge more easily than transition dipole moments, more sensitive to the quality of the wavefunctions, and the inclusion of $\pi \rightarrow \pi^*$ excitations. It also shows that, although double excitations do not play a major qualitative role in the description of low-lying excited states considered here, they certainly have a quantitative influence, with regard to the non-dynamical correlation and to dispersion contributions.

On the basis of detailed cross-comparison of potential energy profiles and oscillator strengths, we conclude that the DFTB-CI provides reasonable excited state potential energy surfaces for these systems. We have shown that it does not only work in the simple sandwich approaches, but that it also provides consistent representation of the PEC in rotated sandwich geometries and also T-shape geometries. We have also shown that fully qualitative and even semi-quantitative consistency can be reached, in concern with the magnitudes and evolution of the splittings of the lower inter-molecular excited states. The fact that DFTB-CI provides overall consistent features shows that it contains the essential ingredients to describe the lowest part of the electronic excited PEC of the inter-molecular systems under consideration. While the oscillator strengths show reasonable qualitative behavior, quantitative analysis reveals the lack of $\pi \rightarrow \pi^*$ excitations. Clearly, for complexes made of non identical systems, one should pay particular attention to possible errors concerned with the relative positions of monomer excitation energies. It should be noted that the present DFTB-CI method involves considerably shorter calculation times with respect to the reference *ab initio* method used. For instance, on an Intel Xeon X5570 2.93 GHz monoprocessor, computing a single geometry of the pyrene dimer cation in the sandwich configuration for 8 states requires about 4.5 seconds with DFTB-CI whereas the calculation time for a single of these states on the same computer is 35 minutes for CAS(15/8)PT2 in basis B1, and 23 hours per state for CAS(1/1)PT2 in basis B3. The most expensive step in DFTB-CI is not the CI but the constrained SCC-DFTB computing the charge localized configuration orbitals.

Obviously, there are various approximations in the present scheme. First, we used the same DFTB parameters, essentially derived for the ground state calculations. Revisitation of the parametrization procedure, involving inclusion of band structure and/or excited states in the fitting targets, or reconsideration of the contraction constraint might be relevant[93] but is clearly beyond the scope of the present work.

As a further application, we have investigated the electronic

spectra of the most stable isomers found for the pyrene dimer and trimer cations. Comparison with previous theoretical data and with experimental data allows to get insight in the electronic structure and spectroscopy of dimer cations. In the trimer case, our results confirm similar findings for naphthalene by Bouvier *et al.* using the VB model[63], namely the charge is not equally shared over the different units. Furthermore, two other isomers exist and are characterized by a dimer core. The present results for thetrimer and the tetramer are in line with the pattern characterizing small rare gas singly charged cluster ions and also with experimental discussions about other PAH cluster cations[17]. It is seen that not only the isomers can be specified by their core geometry and charge patterns, but also by the electronic spectral lines, again in large similarity with rare gas cluster ions.

However, as demonstrated on dimers and except for the ground and first excited sates, HOMO hole monomer-based configurations are not sufficient to quantitatively describe the electronic spectra. When lower energy hole orbitals are included, the DFTB-CI spectra are realistic within a 3 eV window. This is also a window where crossings do happen between bound states correlated with intramonomer excitation and repulsive states characterized by charge transfer excitations. This should affect the photodissociation pattern, at least of naphtalene and pyrene dimer cations, and might affect larger clusters even more.

Acknowledgments

This work was supported by ANR grant ANR-10-BLAN-0501-GASPARIM, "Programme Investissements d'Avenir" ANR-11-IDEX-0002-02 with reference ANR-10-LABX-0037-NEXT and GDR (3533) EMIE. It was granted access to the HPC resources of CALMIP supercomputing center under the allocation 2012-P1042, 2011-P1144, and 2015-P0059.

References

1 M. Rapacioli, C. Joblin and P. Boissel, *Astron. Astrophys.*, 2005, **429**, 193–204.

2 M. Rusyniak, Y. Ibrahim, E. Alsharaeh, M. Meot-Ner and M. El-Shall, *J. Phys. Chem. A*, 2003, **107**, 7656–7666.

3 A. Ławicki, A. I. S. Holm, P. Rousseau, M. Capron, R. Maisonny, S. Maclot, F. Seitz, H. A. B. Johansson, S. Rosén, H. T. Schmidt, H. Zettergren, B. Manil, L. Adoui, H. Cederquist and B. A. Huber, *Phys. Rev. A*, 2011, **83**, 022704–8.

4 M. Schmidt, A. Masson and C. Bréchignac, *Int. J. Mass Spectrom.*, 2006, **252**, 173.

5 P. Bréchignac, M. Schmidt, A. Masson, T. Pino, P. Parneix and C. Bréchignac, *Astron. Astrophys.*, 2005, **442**, 239–247.

6 F. Piuzzi, I. Dimicoli, M. Mons, P. Millié, V. Brenner, Q. Zhao, B. Soep and A. Tramer, *Chem. Phys.*, 2002, **275**, 123–147.

7 H. Sabbah, L. Biennier, S. J. Klippenstein, I. R. Sims and B. R. Rowe, *J. Chem. Phys.Lett.*, 2010, **1**, 2962–2967.

8 F. H. Field, P. Hamlet and W. F. Libby, *J. Am. Chem. Soc.*, 1969, **91**, 2839–2842.

9 J. R. Grover, E. A. Walters and E. T. Hui, *J. Phys. Chem.* , 1987, **91**, 3233–3237.

10 H. Krause, B. Ernstberger and H. J. Neusser, *Chem. Phys. Lett.*, 1991, **184**, 411–417.

11 M. Meot-Ner, P. Hamlet, E. P. Hunter and F. H. Field, *J. Am. Chem. Soc.*, 1978, **100**, 5466–5471.

12 K. Hiraoka, S. Fujimaki, K. Aruga and S. Yamabe, *J. Chem. Phys.*, 1991, **95**, 8413–8418.

13 Y. Ibrahim, E. Alsharaeh, M. Rusyniak, S. Watson, M. M. N. Mautner and M. S. El-Shall, *Chem. Phys. Lett.*, 2003, **380**, 21–28.

14 Y. Inokuchi, K. Ohashi, M. Matsumoto and N. Nishi, *J. Phys. Chem.* , 1995, **99**, 3416–3418.

15 H. Shinohara and N. Nishi, *J. Chem. Phys.*, 1989, **91**, 6743–6751.

16 K. Ohashi, Y. Inokuchi and N. Nishi, *Chem. Phys. Lett.*, 1996, **263**, 167–172.

17 T. Fujiwara and E. C. Lim, *J. Phys. Chem. A*, 2003, **107**, 4381–4386.

18 B. Badger and B. Brocklehurst, *Trans. Faraday Soc.*, 1969, **65**, 2588–2594.

19 I. K. Attah, S. P. Platt, M. M.-N. (Mautner), M. S. El-Shall, R. Peverati and M. Head-Gordon, *J. Phys. Chem. Lett.*, 2015, **6**, 1111–1118.

20 S. Samori, M. Fujitsuka and T. Majima, *Research on Chemical Intermediates*, 2013, **39**, 449–461.

21 H. Haberland, B. von Issendorff, T. Kolar, H. Kornmeier, C. Ludewigt and A. Risch, *Phys. Rev. Lett.*, 1991, **67**, 3290–3293.

22 M. Amarouche, G. Durand and J. P. Malrieu, *J. Chem. Phys.*, 1988, **88**, 1010–1018.

23 M. Grigorov and F. Spiegelman, *Surf. Rev. Lett.*, 1996, **3**, 211–215.

24 F. Gadea and M. Amarouche, *Chem. Phys.*, 1990, **140**, 385.

25 J. Galindez, F. Calvo, P. Paska, D. Hrivnak, R. Kalus and F. X. Gadéa, *Comput. Phys. Comm.*, 2002, **145**, 126–140.

26 F. Calvo, D. Bonhommeau and P. Parneix, *Phys. Rev. Lett.*, 2007, **99**, 083401–4.

27 F. Calvo, J. Galindez and F. X. Gadea, *Phys. Chem. Chem. Phys.*, 2003, **5**, 321–328.

28 F. Calvo, F. X. Gadéa, A. Lombardi and V. Aquilanti, *J. Chem. Phys.*, 2006, **125**, 114307.

29 S. S. Shaik and P. C. Hiberty, *A Chemist's Guide to Valence Bond Theory*, Wiley-Interscience, New Jersey, 2008, p 1–290.

30 A. Dreuw and M. Head-Gordon, *J. Am. Chem. Soc.*, 2004, **126**, 4007–4016.

31 T. S. Chwee, A. B. Szilva, R. Lindh and E. A. Carter, *J. Chem. Phys.*, 2008, **128**, –.

32 J. P. Perdew and A. Zunger, *Phys. Rev. B*, 1981, **23**, 5048—5079.

33 J. Gräfenstein, E. Kraka and D. Cremer, *J. Chem. Phys.*, 2004, **120**, 524–539.

34 T. Tsuneda and K. Hirao, *Wiley Interdisciplinary Reviews: Computational Molecular Science*, 2014, **4**, 375–390.

35 C. Li, X. Zheng, A. J. Cohen, P. Mori-Sánchez and W. Yang, *Phys. Rev. Lett.*, 2015, **114**, 053001.

36 A. Savin, *Recent developments and applications of modern Density Functional Theory*, J. Seminario, Elsevier, Amsterdam,

1996, p. 327–357.
37 J. Toulouse, F. Colonna and A. Savin, *Phys. Rev. A*, 2004, **70**, 062505.
38 L. Goerigk and S. Grimme, *Wiley Interdisciplinary Reviews: Computational Molecular Science*, 2014, **4**, 576–600.
39 T. Kowalczyk, S. R. Yost and T. V. Voorhis, *The Journal of Chemical Physics*, 2011, **134**, –.
40 Y. M. Rhee, T. J. Lee, M. S. Gudipati, L. J. Allamandola and M. Head-Gordon, *Proc. Natl. Acad. Sci. Unit. States Am.*, 2007, **104**, 5274.
41 E. Miyoshi, T. Ichikawa, T. Sumi, Y. Sakai and N. Shida, *Chem. Phys. Lett.*, 1997, **275**, 404–408.
42 E. Miyoshi, N. Yamamoto, M. Sekiya and K. Tanaka, *Mol. Phys.*, 2003, **101**, 227–232.
43 P. A. Pieniazek, A. I. Krylov and S. E. Bradforth, *J. Chem. Phys.*, 2007, **127**, 044317–16.
44 E. S. Kryachko, *Int. J. Quant. Chem.*, 2007, **107**, 2741–2755.
45 P. A. Pieniazek, S. E. Bradforth and A. I. Krylov, *J. Chem. Phys.*, 2008, **129**, 074104–11.
46 D. Porezag, T. Frauenheim, T. Köhler, G. Seifert and R. Kaschner, *Phys. Rev. B*, 1995, **51**, 12947–12957.
47 G. Seifert, D. Porezag and T. Frauenheim, *Int. J. Quant. Chem.*, 1996, **58**, 185–192.
48 M. Elstner, D. Porezag, G. Jungnickel, J. Elsner, M. Haugk, T. Frauenheim, S. Suhai and G. Seifert, *Phys. Rev. B*, 1998, **58**, 7260–7268.
49 T. Frauenheim, G. Seifert, M. Elsterner, Z. Hajnal, G. Jungnickel, D. Porezag, S. Suhai and R. Scholz, *Phys. Stat. Solidi (b)*, 2000, **217**, 41–62.
50 T. Frauenheim, G. Seifert, M. Elstner, T. Niehaus, C. Köhler, M. Amkreutz, M. Sternberg, Z. Hajnal, A. D. Carlo and S. Suhai, *J. Phys. Cond. Mat.*, 2002, **14**, 3015.
51 A. Oliveira, G. Seifert, T. Heine and H. duarte, *J. Braz. Chem. Soc.*, 2009, **20**, 1193–1205.
52 T. A. Niehaus, S. Suhai, F. Della Sala, P. Lugli, M. Elstner, G. Seifert and T. Frauenheim, *Phys. Rev. B*, 2001, **63**, 085108–9.
53 N. Lutsker, Aradi, arXiv:1504.00243v1.
54 P. Baltzer, L. Karlsson, B. Wannberg, G. Öhrwall, D. Holland, M. MacDonald, M. Hayes and W. von Niessen, *Chemical Physics*, 1997, **224**, 95 – 119.
55 F. Salama and L. J. Allamandola, *J. Chem. Phys.*, 1991, **94**, 6964–6977.
56 D. Romanini, L. Biennier, F. Salama, A. Kachanov, L. J. Allamandola and F. Stoeckel, *Chem. Phys. Lett.*, 1999, **303**, 165–170.
57 T. Pino, N. Boudin and P. Bréchignac, *J. Chem. Phys.*, 1999, **111**, 7337–7347.
58 T. Bally, C. Carra, M. P. Fulscher and Z. Zhu, *J. Chem. Soc., Perkin Trans. 2*, 1998, 1759–1766.
59 S. Hirata, M. Head-Gordon, J. Szczepanski and M. Vala, *The Journal of Physical Chemistry A*, 2003, **107**, 4940–4951.
60 F. Negri and M. Z. Zgierski, *The Journal of Chemical Physics*, 1994, **100**, 1387–1399.
61 M. Vala, J. Szczepanski, F. Pauzat, O. Parisel, D. Talbi and Y. Ellinger, *The Journal of Physical Chemistry*, 1994, **98**, 9187–9196.
62 R. Boschi and W. Schmidt, *Tetrahedron Letters*, 1972, **13**, 2577–2580.
63 B. Bouvier, V. Brenner, P. Millié and J.-M. Soudan, *J. Phys. Chem. A*, 2002, **106**, 10326–10341.
64 M. Rapacioli and F. Spiegelman, *Eur. Phys. J. D*, 2009, **52**, 55–58.
65 M. Rapacioli, F. Spiegelman, A. Scemama and A. Mirtschink, *J. Chem. Theor. Comput.*, 2011, **7**, 44–55.
66 M. Rapacioli, A. Simon, L. Dontot and F. Spiegelman, *Phys. Stat. Solidi (b)*, 2012, **249**, 245–258.
67 Q. Wu and T. Van Voorhis, *J. Chem. Phys.*, 2006, **125**, 164105–9.
68 Q. Wu, C.-L. Cheng and T. Van Voorhis, *J. Chem. Phys.*, 2007, **127**, 164119–9.
69 A. L. Thompson and T. J. Martinez, *Faraday Discuss.*, 2011, **150**, 293–311.
70 M. Elstner, P. Hobza, T. Frauenheim, S. Suhai and E. Kaxiras, *J. Chem. Phys.*, 2001, **114**, 5149–5155.
71 L. Zhechkov, T. Heine, S. Patchovskii, G. Seifert and H. Duarte, *J. Chem. Theor. Comput.*, 2005, **1**, 841–847.
72 M. Rapacioli, F. Spiegelman, D. Talbi, T. Mineva, A. Goursot, T. Heine and G. Seifert, *J. Chem. Phys.*, 2009, **130**, 244304–10.
73 J. Kalinowski, B. Lesyng, J. Thompson, C. Cramer and D. Truhlar, *J. Phys. Chem. A*, 2004, **108**, 2545–2549.
74 Y. Yang, H. Yu, D. Uork, Q. Cui and M. Elstner, *J. Phys. Chem. A*, 2007, **111**, 10861–10873.
75 *The hopping and overlap integrals of the atomic basis $t(R)$ are modified for $R > 4$, with R in Angströms as :*

$$t(\tilde{R}) = (1+a(R)) * t(\lambda R) \quad (9)$$

$$a(R) = 0.5(R-4)^3 * \exp(-1.35(R-4)) \quad (10)$$

with λ =1 and 0.98 for CC, CH respectively.
76 C. Iftner, A. Simon, K. Korchagina, M. Rapacioli and F. Spiegelman, *J. Chem. Phys.*, 2014, **140**, 034301–1.
77 T. Heine, M. Rapacioli, S. Patchkovskii, J. Frenzel, A. Koster, P. Calaminici, H. A. Duarte, S. Escalante, R. Flores-Moreno, A. Goursot, J. Reveles, D. Salahub and A. Vela, deMon-Nano Experiment 2009, http://physics.jacobs-university.de/theine/research/deMon/.
78 F. Aquilante, L. De Vico, N. Ferré, G. Ghigo, P.-å. Malmqvist, P. Neogrády, T. B. Pedersen, M. Pitoňák, M. Reiher, B. O. Roos, L. Serrano-Andrés, M. Urban, V. Veryazov and R. Lindh, *Journal of Computational Chemistry*, 2010, **31**, 224–247.
79 G. Karlström, R. Lindh, P.-Å. Malmqvist, B. O. Roos, U. Ryde, V. Veryazov, P.-O. Widmark, M. Cossi, B. Schimmelpfennig, P. Neogrady and L. Seijo, *Computational Materials Science*, 2003, **28**, 222–239.
80 V. Veryazov, P.-O. Widmark, L. Serrano-Andrés, R. Lindh and B. O. Roos, *International Journal of Quantum Chemistry*, 2004,

100, 626–635.

81 B. O. Roos, R. Lindh, P.-Å. Malmqvist, V. Veryazov and P.-O. Widmark, *The Journal of Physical Chemistry A*, 2003, **108**, 2851–2858.

82 P.-O. Widmark, P.-Å. Malmqvist and B. Roos, 1990, **77**, 291–306.

83 H. J. Werner, *Mol. Phys.*, 1996, **89**, 645.

84 K. Andersson, P.-A. Malmqvist and B. O. Roos, *J. Chem. Phys.*, 1992, **96**, 1218–1226.

85 K. Andersson, P. A. Malmqvist, B. O. Roos, A. J. Sadlej and K. Wolinski, *J. Phys. Chem.*, 1990, **94**, 5483–5488.

86 A. M. Tokmachev, M. Boggio-Pasqua, M. J. Bearpark and M. A. Robb, *The Journal of Physical Chemistry A*, 2008, **112**, 10881–10886.

87 S. Hirata, T. J. Lee and M. Head-Gordon, *The Journal of Chemical Physics*, 1999, **111**, 8904–8912.

88 G. Malloci, G. Mulas and C. Joblin, *A&A*, 2004, **426**, 105–117.

89 F. Negri and M. Z. Zgierski, *The Journal of Chemical Physics*, 1994, **100**, 1387–1399.

90 Z. H. Khan, *Spectrochimica Acta Part A: Molecular Spectroscopy*, 1989, **45**, 253–270.

91 T. Kubař, P. B. Woiczikowski, G. Cuniberti and M. Elstner, *J. Phys. Chem. B*, 2008, **112**, 7937–7947.

92 F. Calvo, *J. Chem. Phys.*, 2005, **123**, 124106–7.

93 M. Wahiduzzaman, A. F. Oliveira, P. Philipsen, L. Zhechkov, E. van Lenthe, H. A. Witek and T. Heine, *J. Chem. Theor. Comput.*, 2013, **9**, 4006–4017.